Heliyon 9 (2023) e20430

Contents lists available at ScienceDirect

Heliyon

journal homepage: www.cell.com/heliyon

Exploring mesoporous silica nanoparticles as oral insulin carriers: *In-silico* and *in vivo* evaluation

Ehsan Salarkia [a], Mahdis Mehdipoor [b], Elahe Molaakbari [c], Ahmad Khosravi [a,*], Mohammad Reza Sazegar [b,**], Zohreh Salari [d], Iman Rad [e], Shahriar Dabiri [e], Siyavash Joukar [f], Iraj Sharifi [a], Guogang Ren [g]

[a] *Leishmaniasis Research Center, Kerman University of Medical Sciences, Kerman, Iran*
[b] *Faculty of Chemistry, North Tehran Branch, Islamic Azad University, Hakimiyeh, Tehran, Iran*
[c] *Department of Chemistry, Shahid Bahonar University of Kerman, Kerman, Iran*
[d] *Department of Obstetrics and Gynecology, Afzalipour School of Medicine, Kerman University of Medical Sciences, Kerman, Iran*
[e] *Afzalipour School of Medicine & Pathology and Stem Cells Research Center, Kerman University of Medical Sciences, Kerman, Iran*
[f] *Neuroscience Research Center, Institute of Basic and Clinical Physiology Sciences, Department of Physiology and Pharmacology, Afzalipour Faculty of Medicine, Kerman University of Medical Sciences, Kerman, Iran*
[g] *School of Engineering and Computer Science, University of Hertfordshire, Hatfield, AL10 9AB, UK*

ARTICLE INFO

Keywords:
Mesoporous silica nanoparticles
Oral insulin
Diabetic rat
PEG
In-silico

ABSTRACT

The advancements in nanoscience have brought attention to the potential of utilizing nanoparticles as carriers for oral insulin administration. This study aims to investigate the effectiveness of synthesized polymeric mesoporous silica nanoparticles (MSN) as carriers for oral insulin and their interactions with insulin and IR through *in-silico* docking. Diabetic rats were treated with various MSN samples, including pure MSN, Amin-grafted MSN/PEG/Insulin (AMPI), Al-grafted MSN/PEG/Insulin (AlMPI), Zinc-grafted MSN/PEG/Insulin (ZNPI), and Co-grafted MSN/PEG/Insulin (CMPI). The nanocomposites were synthesized using a hybrid organic-inorganic method involving MSNs, graphene oxide, and insulin. Characterization of the nanocomposites was conducted using X-ray diffraction (XRD), Fourier-transform infrared (FTIR) spectroscopy, and scanning electron microscopy (SEM). *In vivo* tests included the examination of blood glucose levels and histopathological parameters of the liver and pancreas in type 1 diabetic rats. The MSN family demonstrated a significant reduction in blood glucose levels compared to the diabetic control group ($p < 0.001$). The synthesized nanocomposites exhibited safety, non-toxicity, fast operation, self-repairing pancreas, cost-effectiveness, and high efficiency in the oral insulin delivery system. In the *in-silico* study, Zn-grafted MSN, Co-grafted MSN, and Al-grafted MSN were selected. Docking results revealed strong interactions between MSN compounds and insulin and IR, characterized by the formation of hydrogen bonds and high binding energy. Notably, Co-grafted MSN showed the highest docking scores of −308.171 kcal/mol and −337.608 kcal/mol to insulin and IR, respectively. These findings demonstrate the potential of polymeric MSN as effective carriers for oral insulin, offering promising prospects for diabetes treatment.

* Corresponding author.7616914111, Iran.
** Corresponding author.
E-mail addresses: khosraviam@yahoo.com (A. Khosravi), m_r_sazegar@yahoo.com (M.R. Sazegar).

https://doi.org/10.1016/j.heliyon.2023.e20430
Received 11 May 2023; Received in revised form 23 September 2023; Accepted 25 September 2023
Available online 26 September 2023
2405-8440/© 2023 The Authors. Published by Elsevier Ltd. This is an open access article under the CC BY-NC-ND license (http://creativecommons.org/licenses/by-nc-nd/4.0/).

1. Introduction

According to the 10th edition of the International Diabetes Federation (IDF) Diabetes Atlas in 2022, there are over 473 million people worldwide suffering from diabetes mellitus (DM) [1]. The primary goal in managing DM is to regulate blood glucose levels within the normal range of 70–140 mg/dL [2,3].

Insulin administration is crucial for patients with diabetes mellitus (DM) to effectively manage their condition. Despite advancements in drug delivery systems, subcutaneous injection of insulin remains the primary and widely used approach, with no equally effective alternative method currently available [4]. Various non-invasive drug delivery strategies have emerged, including the lung or nasal route and micro-array patches. However, these alternative methods of insulin injection face challenges such as low permeability, high costs, and immune reactions, leading to limited success [5].

Oral drug delivery is preferred due to its non-invasiveness, eliminating the need for injections and reducing the risk of infectiona and can be a suitable alternative to insulin injections for various reasons, including non-invasive administration, improved glycemic control, reduced risk of hypoglycemia, simplified treatment regimen, and expanded accessibility. However, the protein structure of insulin is vulnerable to stomach acid, which can reduce its effectiveness. The use of suitable carriers for insulin transfer can improve the effectiveness of this treatment method. It allows for absorption through the physiological pathway, resulting in increased effectiveness. However, there are challenges associated with oral insulin delivery. Insulin, being a protein, needs to pass through the intestinal mucosa using various mechanisms to function properly. Insulin's high molecular weight and lack of lipophilicity make it more difficult to absorb compared to other oral drugs. Previous studies have shown that the systemic circulation of orally administered insulin is typically less than 10%, with less than 0.5% being absorbed [6,7]. Achieving a stable formulation of oral insulin could provide a viable alternative to injections, but it would require significant investment and commercial development. Additionally, the cost difference between the two methods of drug administration, including the preparation of injection vials and supplies, as well as the need for multiple daily injections for some patients, should be considered. Factors such as effectiveness, convenience, and safety will also play a crucial role in determining the overall value proposition of oral insulin [6,8].

Various carriers, including hydrogels, liposomes, and nanoparticles, have been utilized in oral protein anddrug delivery Nano-sized structures are preferred in oral delivery systems due to their enhanced cell absorption and epithelial penetration [9,10].

Nanoparticles can improve protein stability and prolong the duration of drug action when used as a delivery system. Mesoporous silica nanoparticles (MSN) possess desirable properties such as large pore size, high surface area, physical stability, non-toxicity, and solvent compatibility, making them highly promising in drug delivery systems [11–13]. Researchers have modified pure MSN by incorporating natural polymers like chitosan and agar for insulin delivery. These nanocomposites offer protection for the drug and facilitate easy absorption through the intestinal mucosa [14,15].

Moreover, computational simulations using molecular docking procedures can provide valuable insights into the specificity of binding sites and predict interactions between ligands and proteins. *In-silico* methods serve as both an alternative and complement to in vitro studies, offering detailed information about molecular interactions that may not be feasible to observe experimentally [16]. Molecular docking studies play a crucial role in elucidating the relationship between ligand structure and protein function, as well as in interpreting drug delivery processes and therapeutic effectiveness.

The biological actions of insulin occur through its interaction with the insulin receptor (IR), a transmembrane glycoprotein belonging to the receptor tyrosine kinase family, which plays a vital role in signal transduction [17,18]. The IR is responsible for regulating glucose accessibility in cells. When insulin levels decrease, cells, particularly those with high insulin sensitivity, rely on lipids that can directly enter the cells without requiring membrane transport. The interaction between insulin and the IR involves two distinct binding modes: low-affinity and high-affinity, with negative cooperativity observed between two equivalent binding pockets [17,19]. Activation of the IR involves the compaction of the insulin-receptor complex, autophosphorylation of cytoplasmic kinases, and initiation of downstream signaling cascades. Consequently, all domains of the IR hold potential as targets for drug development [20].

In the quest for an effective oral insulin delivery system, researchers have developed enteric spherical nanomaterials using MSN as drug carriers. These nanocomposites were evaluated for their therapeutic effects and safety by measuring blood glucose levels and examining liver histopathological findings in diabetic rats. Additionally, the nanocomposite structures were analyzed using the Docking analysis program to gain theoretical insights.

2. Material and methods

2.1. Material

All materials including Tetraethylorthosilicate (TEOS, purity 99%), cetyltrimethylammonium bromide (CTAB, 98%), 3-Aminopropyltriethoxysilane (APTES, 99%), ethanol (96%), polyethylene glycol (PEG>5 kDa), ammonia solution (28%), sodium aluminate, cobalt nitrate hexahydrate, and Zinc nitrate hexahydrate were purchased from Merck Company, German. STZ was purchased from Sigma-Aldrich, Germany (Cas no. 18883-66-4), and the insulin was purchased from Daru Pakhsh Co., Tehran, Iran.

2.2. Synthesis of the nanomaterials

All methods of the synthesis of the MSN, AMPI, AlMPI, ZMPI, and CMPI nanocomposites were described in the supplementary materials information section.

2.3. Characterization of the nanocomposites

The pristine MSN and the AMPI, AlMPI, ZMPI, and CMPI nanocomposites were subjected to various characterization techniques to assess their properties. The following analyses were conducted: Fourier-transform infrared (FTIR) spectroscopy, X-ray diffraction (XRD) pattern analysis, scanning electron microscopy (SEM) imaging, zeta potential measurement, and nitrogen adsorption-desorption analysis. The crystallinity of the catalysts was determined using a Bruker Advance D8 X-ray powder diffractometer with Cu Kα ($\lambda = 1.5418$ Å) radiation as the diffracted monochromatic beam. The measurements were performed at 40 kV and 40 mA. Nitrogen physisorption analysis was carried out using a Quantachrome Autosorb-1 instrument at a temperature of 77 K. Before the measurement, the sample was evacuated at 573 K for 3 h. The morphology and average particle size of the catalysts were evaluated using a scanning electron microscope (SEM), specifically a JEOL JSM-6701 F model. Prior to SEM observation, the samples were coated with Pt using a sputtering instrument. Fourier-transform infrared (FTIR) measurements were conducted using an Agilent Carry 640 FTIR spectrometer. Zeta potential measurements were performed on a Zetasizer Nano ZS instrument (Malvern Instruments, Westborough, MA) using a Phosphate-buffered saline (PBS). Backscattering detection was employed, and the measurements were taken at an angle of 173°.

2.4. In vivo assay

2.4.1. Animals

This study was conducted in accordance with the ethical standards and approved by the Institutional Review Board with the code of IR.KMU.REC.1398.324. A total of 49 adult male Wistar rats weighing between 220 and 250 g were obtained from the Animal Farm of Kerman, Iran. The rats were housed in a controlled environment with a 12-h light/dark cycle and maintained at a temperature of 25 ± 2 °C.

2.4.2. Induction of diabetes

Diabetes was induced in rats by injection of Streptozotocin (STZ, Sigma) (60 mg/kg subcutaneous injection) in a 10 mM citrate buffer (10 mM at pH 4.5). For confirmation of diabetic rats after 72 h, FBS was checked by glucose meter (Accuchek; Roche, Germany). Rats with FBS levels beyond 250 mg/dl were regarded as diabetic.

2.4.3. Experimental groups

To investigate the effects of oral insulin on FBS in diabetic rats, animals were randomly divided into 7 treatment groups (7 animals in each), including:

Group 1. The control group: received citrate buffer (10 mM at pH 4.5, IP)

Group 2. The diabetic control group (STZ): diabetic rats induced by STZ received no treatment.

Group 3. Insulin group (INS): a diabetic group treated with regular insulin (5 IU/Kg) daily, subcutaneous injection after eating) [21].

Group 4. The AlMPI group: diabetic group treated with oral insulin MSN capsulated with NH_2-AlMPI (30 IU/kg, by gavage)

Group 5. ZMPI group: diabetic group treated with oral insulin MSN capsulated with NH_2-ZMPI (30 IU/kg, by gavage)

Group 6. MCPI group: diabetic group treated with oral insulin MSN capsulated with NH_2-MCPI (30 IU/kg, by gavage)

Group 7. MNPI group: diabetic group treated with oral insulin MSN capsulated with NH_2-MNPI (30 IU/kg [29], by gavage)

2.4.4. Long-term efficacy of the MSN for the oral insulin

To investigate the long-term efficacy and toxicity of the nanoparticles, four groups of diabetic rats were established: a control group, and groups treated with AlMPI, MCPI, MNPI, and ZNPI. The rats in each group were orally administered either saline (control) or an MSN form of insulin daily for a duration of 10 days. Throughout the study, the rats' body weight, as well as their daily food and water intake, were monitored. Fasting blood glucose levels were measured at various time points: 0, 30, 60, 120, 180, and 360 min after the insulin administration. Blood samples, approximately 0.05 mL in volume, were collected from the tail vein for glucose analysis. An ACCU-CHEK Glucose Advantage Meter (Roche, Munich, Germany) was used to measure the blood glucose levels. Following the 10-day treatment period, the rats were euthanized by administering a mixture of Ketamine and Xylazine (100/10 mg/kg, i.p.). Blood samples were collected from the vena cava, and the pancreases and livers were removed and fixed in 10% neutral buffered formalin for subsequent histopathological examination. The formalin-fixed samples were processed using conventional paraffin embedding techniques. Thin slices, approximately 5 μm thick, were obtained from the samples and stained with Hematoxylin and Eosin (H&E) for histopathological analysis. The stained samples were then examined using a light microscope under 40× magnification to assess any histological changes or abnormalities.

2.4.5. Liver enzymatic measurement

The blood samples were centrifuged for 5 min at 4-6 °C and 2500 rpm. According to the manufacturer's instructions, the levels of ALT and AST were measured by radioimmunoassay the using ELISA technique using a commercial kit (Pars Azmoon, Iran).

2.4.6. Statistical analysis

Statistical analysis was conducted using SPSS software version 24.0 (SPSS Inc., Chicago, USA) by using repeated measure ANOVA followed by post hoc Tukey HSD test. The graph was prepared using Graph Pad Prism version 8.0 (Graph Pad Software, San Diego,

USA). Data were expressed as means ± S.D. (standard deviation). The level of significance was taken at $p < 0.05$.

2.5. In-silico assay

2.5.1. Molecular docking

In this study, molecular docking was employed using Molegro Virtual Docker software 6.0 (MVD) to investigate the interactions between the Amin-grafted MSN, Al-grafted MSN, Zn-grafted MSN, and Co-grafted MSN nanoparticles with insulin and insulin receptor (IR). Molecular docking is a valuable tool for predicting the binding affinity and identifying the binding site of ligands within proteins [22].

MVD was chosen for its widespread usage and effectiveness in determining ligand-protein interactions, with an accuracy rate of 87% that surpasses many other similar tools. Standard procedures were followed during the docking process, as described in Refs. [23–25].

To conduct the docking study, the proteins involved in the mechanism of action of insulin and IR were utilized. The X-ray crystallographic 3D structural segments of insulin (PDB ID: 6JK8) and IR (PDB ID: 4ZXB) were obtained from the Protein Data Bank (PDB) maintained by the RCSB (Research Collaboratory for Structural Bioinformatics) and downloaded for use in this study. For more detailed information on the MVD process, as well as protein and ligand preparation, please refer to the supplementary material provided with the study.

3. Results and discussion

3.1. Nanocomposites characterization

The pure MSN was prepared through the sol-gel method using TEOS, CTAB, APTES, and the MCPI, MNPI, AlMPI, and ZNPI nanocomposites were synthesized from the initial MSN (supplementary material). Fig. 1A shows the XRD patterns of the MSN nanoparticles and all the MCPI, MNPI, AlMPI, and ZNPI nanocomposites. The pure MSN nanoparticles exhibited three diffraction peaks, including an intense peak of 100 and two smaller peaks of 110, at low angles in the range of 2.10–5.70°. These diffraction peaks indicated an ordered 2D hexagonal (p6mm) structure with a d100-spacing of approximately 3.6 nm [13].

The incorporation of the amine group, aluminum, cobalt, and zinc with PEG and insulin molecules in the pure MSN sample resulted in MNPI, AlMPI, MCPI, and ZNPI, respectively, and decreased the order of the mesoporous structure compared to the pure MSN structure [26]. The presence of these metals with larger radii than Si atoms, along with the bulky organic molecules, caused alterations in the ordered plates of the pure MSN, leading to observable shifts in the peak of 100 [27,28]. Consequently, the loading of these

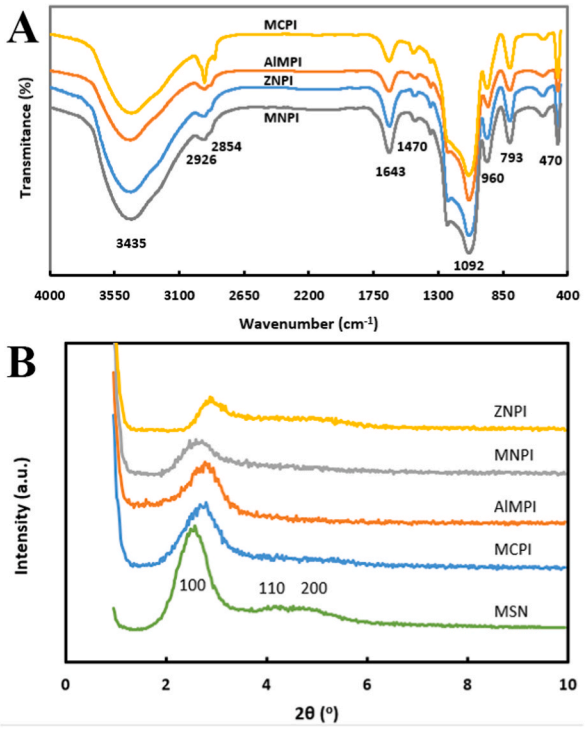

Fig. 1. (A) XRD patterns in a low degree at 0-10°, (B) Fourier transform infrared (FTIR(spectra of the MSN, MNPI, AlMPI, ZNPI, MCPI nanocomposites.

components significantly reduced all peaks of 100, 110, and 200 in the synthesized nanocomposites, resulting in a reduction in mesoporous crystallinity.

The FTIR spectra of the MNPI, ZNPI, AlMPI, and MCPI samples range from 400 to 4000 cm^{-1} (Fig. 1B). The strong and broad peaks at the range of 3050–3600 cm^{-1} are attributed to hydrogen bonding due to the hydroxyl, amine, or silanol groups in the synthesized nanomaterial structures [26]. The presence of nitrogen containers produced sharper peaks in the 3435 cm^{-1}, these peaks overlapped with the silanol or hydroxyl groups. The results exhibited the presence of the zinc and aluminum metals in the samples in comparison to the sample without these metals resulting in a decrease in the intensity of the broad peak of 3435 cm^{-1} due to the formation of Zn–*O*–Si or Al–*O*–Si bands in their frameworks which caused a decrease in the number of the H-bonding.

Loading of CTAB in the MSN drastically reduced the height of the broad peak, which is evidence of the condensation reaction of the OH groups of MSN with the alcoholic groups of CTAB that deceased the hydrogen bonding numbers. Two vibration bands at the regions of 1092 and 470 cm^{-1} are attributed to the asymmetric and symmetric Si–*O*–Si stretching vibration, respectively. Also, two peaks at 793 and 1643 cm^{-1} correspond to the Si–*O*–Si bending vibration, respectively [26]. However, the vibration bands related to the presence of Al and Zn overlapped with the Si–O bands at 470 cm^{-1}. In addition, two bands at the regions of 2926 and 2854 cm^{-1} were assigned to the C–H stretching due to the presence of PEG, CTAB, and insulin molecules in these nanocomposite structures.

Results of the XRD patterns of the MSN, MNPI, AlMPI, ZNPI, and MCPI nanocomposites revealed the reduction in the order of MSN structure due to the amination of MSN and also loading of aluminum, zinc, and cobalt with PEG and insulin in the MSN structure. Therefore, the crystallinity of the nanocomposites was decreased due to the introduction of metals and bulky organic compounds [26].

The physical properties resulting from nitrogen adsorption-desorption showed a decrease in the surface area, pore size, and volume of the composites after loading with metals and organic compounds. This phenomenon is attributed to the plugging of MSN pores and the occupation of the surface by metal species, PEG, and insulin [13].

SEM and TEM images revealed the spherical shape of the nanoparticles in the MNPI, AlMPI, ZNPI, and MCPI nanocomposites, with particle sizes ranging from 70 to 150 nm (Fig. 2A-J). The SEM results displayed uniform spherical particles with sizes of 70–150 nm (Fig. 2A-E), indicating that the loading of metals, PEG, and insulin altered the shape of the nanoparticles from spherical to broad and large spherical structures. TEM images showed an ordered two-dimensional hexagonal structure for pure MSN (Fig. 2F), while the loading of amine groups, PEG, and insulin led to a porous structure with large pores (Fig. 2G). TEM images of samples containing metals exhibited worm-like structures (Fig. 2H-J).

Table 1 presented the physical properties of MSN, MNPI, AlMPI, MCPI, and ZNPI samples. The surface area decreased from 995 m2g to 1 for MSN to 472, 316, 270, and 226 m2g-1 for AlMPI, MCPI, MNPI, and ZNPI composites, respectively, indicating less porous structures. Consequently, the pore volume and size of the synthesized nanocomposites decreased, possibly due to pore plugging by metals and PEG molecules. The pore volume decreased from 0.84 cm3g to 1 for MSN to 0.17 cm3g-1 for the ZNPI composite [28], while the pore size decreased from 3.37 nm for MSN to 2.43 nm for the ZNPI composite. This reduction in pore size is also attributed to the loading of Al, Zn, and Co metals with PEG molecules into the MSN structure.

These nanocomposites exhibited larger spherical structures due to the loading of metals and bulky organic molecules. Additionally, FTIR spectroscopy of the synthesized nanocomposites confirmed the presence of amine groups, Si–*O*-M bond formation (M representing metal atoms), and the loading of PEG and insulin molecules.

3.1.1. Zeta potential (ζ) measurement of the nanocomposites

The zeta potential (ζ) of the synthesized nanocomposites is shown in Fig. 3. The zeta potential of the pure MSN changed after loading metals, amine groups, PEG, and insulin. The pure MSN exhibited a negative zeta potential of −16.5 mV, while grafting amine groups, PEG, and insulin in the MSN structure reduced the zeta potential value to −4.5 mV. Insulin and PEG showed zeta potential values of −21.4 and −24 mV, respectively.

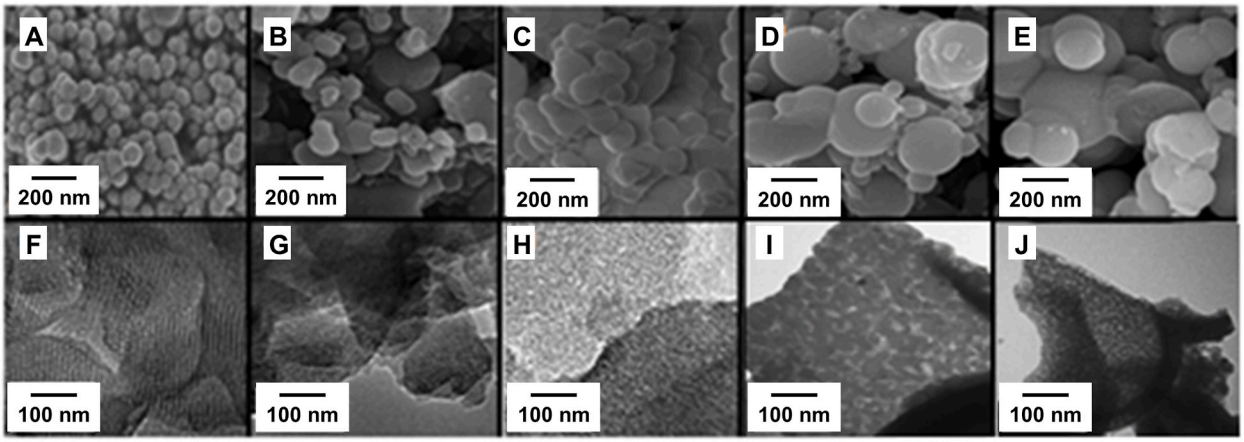

Fig. 2. SEM and TEM images of (A,F) Mesoporous silica nanoparticles (MSN); (B,G) MNPI; (C,H) AlMPI; (D,L) ZNPI; (E,K) MCPI.

Table 1
Physical characteristics of the MSN, MNPI, AlMPI, MCPI, and ZNPI samples.

Sample	S (m^2g^{-1})	V_p (cm^3g^{-1})	W (nm)
MSN	995	0.84	3.37
AlMPI	472	0.29	2.88
MCPI	316	0.23	2.45
MNPI	270	0.18	2.61
ZNPI	226	0.17	2.43

S, BET surface area (m^2g^{-1}) obtained from N_2 adsorption; V_p, total pore volume (cm^3g^{-1}); W, pore size (nm) obtained from BJH method.

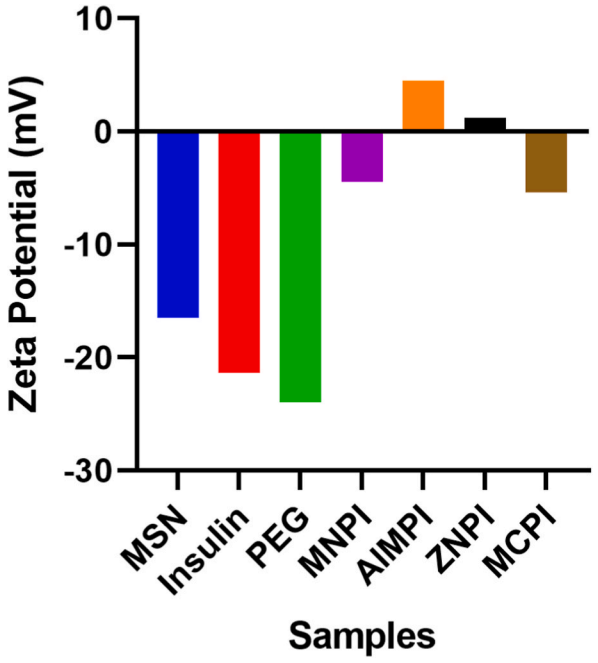

Fig. 3. Zeta potential (ζ) values of the MSN, Insulin, PEG, MNPI, AlMPI, ZNPI, and MCPI.

Grafting the amine group in the pure MSN (referred to as MSN-NH2) yielded a positive zeta potential value of 17.3 mV (not shown). Comparing the zeta potential values of pure MSN, insulin, PEG, and MSN-NH2 revealed that the negative zeta potential values of MSN, insulin, and PEG outweighed the positive charge of 17.3 mV, resulting in a negative zeta potential for the MNPI nanocomposite.

The incorporation of metals such as Al, Zn, and Co in the MSN, along with PEG and insulin, altered the zeta potential values to negative and positive charges. The AlMPI and ZNPI nanocomposites exhibited positive charges of 4.5 and 1.2, respectively, while MCPI showed a negative charge of −5.4 mV. This alteration from negative to positive zeta potential values indicated interactions between the MSN surface and metal ions, followed by PEG and insulin.

The presence of these metal ions in the MSN structure resulted in electrostatic attraction between the positive charge of the modified MSN surface and the negative charges of insulin and PEG molecules. The higher zeta potential of the AlMPI sample can be attributed to the electronic nature of Al3+ ions, which possess a higher positive charge compared to Zn2+ and Co2+ ions. Therefore, it was expected that AlMPI would exhibit a higher zeta potential, confirming that trivalent metals bind more strongly to insulin and PEG [29,30]. Scheme 1 depicts the flowchart of the synthesis of the nanocomposites MNPI, AlMPI, ZNPI, and MCPI.

3.2. The pharmacological effects

The goal of oral insulin is to deliver insulin to the body via the digestive system rather than through injections. If successful, oral insulin could provide a more convenient and potentially less invasive alternative to subcutaneous insulin injections. The pharmacological effects of oral insulin would ideally mimic those of subcutaneous insulin injections. These effects include: blood glucose lowering, glycemic control, mealtime glucose and metabolism regulation.

The pharmacological effects of insulin and MSN forms of oral insulin were evaluated in fasted diabetic rats. After administering the drugs, the fasting blood glucose of each rat was examined every 30 min for 6 h. The observed fasting blood glucose levels showed that in the insulin group, the blood glucose level decreased from 415.57 ± 20.29 mg/dl at the start of treatment to 169.00 ± 18.43 mg/dl after 8 h. We observed a decrease in blood glucose levels in all MSN oral groups (MNPI 413.71 ± 22.14 mg/dl to 274.28 ± 12.98 mg/dl, ZNPI 406.00 ± 15.27 mg/dl to 251.71 ± 12.21 mg/dl, AlMPI 404.00 ± 15.91 mg/dl to 251.85 ± 11.33 mg/dl, and MCPI 418.42 ±

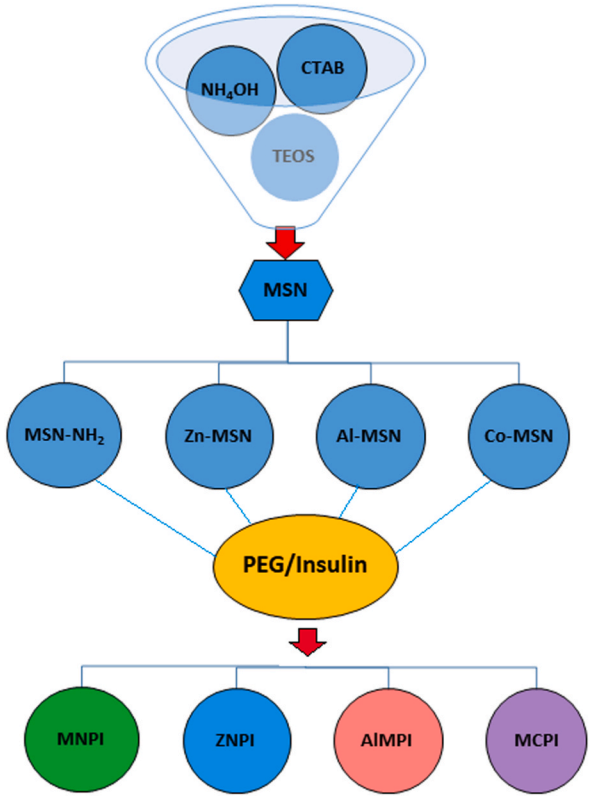

Scheme 1. Flowchart of the synthesis of the nanocomposites MNPI, AlMPI, ZNPI, and MCPI.

10.90 mg/dl to 256.71 ± 13.90 mg/dl). All of these glucose levels were significantly lower than the results of the STZ group (418.00 ± 11.19 to 366.00 ± 10.72) ($p < 0.001$); however, they were higher than the glucose levels in the insulin group ($p < 0.05$).

To evaluate the long-term outcomes of drug use, different forms of MSN insulin were orally administered to diabetic rats for 10 days. Over the course of the 10 days, water and food intake differed between the STZ group and the other groups ($P < 0.001$); however, these parameters were similar among the treated groups (Fig. 4A and B). Additionally, the body weights of the treated groups (including MSN and insulin) showed a trend of weight gain, while the STZ group showed a trend of weight loss (Fig. 4C).

In the insulin group, the fasting blood glucose level decreased from 413.57 ± 16.57 mg/dl at the beginning of treatment to 234.71 ± 14.64 mg/dl at the end of the 10-day treatment period. Lower fasting blood glucose levels were also observed in the MSN oral groups (MNPI 413.71 ± 22.15 mg/dl to 252.86 ± 6.36 mg/dl, ZNPI 404.57 ± 13.49 mg/dl to 243.71 ± 4.39 mg/dl, AlMPI 408.57 ± 16.26 mg/dl to 251.00 ± 12.49 mg/dl, and MCPI 417.86 ± 10.88 mg/dl to 254.57 ± 12.92 mg/dl), which significantly differed from the insulin group ($p < 0.001$). In the STZ group, the fasting blood glucose level did not show any significant difference over the 10 days (416.86 ± 6.28 mg/dl at the beginning and 426.71 ± 8.36 mg/dl at the end), while all other groups showed a significant difference compared to the STZ group ($p < 0.001$)(Fig. 4D). We demonstrated that oral administration of MSN insulin had no effects on the serum biochemical levels of ALT and AST in the liver of STZ-induced diabetic rats (Fig. 4E and F).

To investigate the long-term effects of nanoparticles on organs, we studied the histopathology of the pancreas and liver tissues in the animal groups. In the control group, the liver tissues appeared normal with regular plates, portal spaces, and sinusoids (Fig. 5I(A)). The STZ group showed hepatocytes with hydropic degenerative changes and focal necrotic changes. Mild inflammatory cell infiltration was also noted (Fig. 5I(B)). The insulin group exhibited hepatocytes with dispersed degenerative changes and occasional apoptotic cells (Fig. 5I(C)). The MNPI group exhibited prominent sinusoidal congestion and dispersed mononuclear cell infiltration in the portal space (Fig. 5I(D)). In the AlMPI group, liver cells displayed degenerative changes, apoptotic cells, and slight mononuclear cell infiltration in portal spaces (Fig. 5I(E)). The ZNPI group showed multifocal mononuclear cell infiltration in the parenchyma along with degenerative changes (Fig. 5I(F)). The MCPI group showed hepatocytes with congested sinusoids and an appearance of almost-normal hepatocytes and portal spaces (Fig. 5I(G)).

Regarding the pancreas tissues, the control group displayed normal acini ducts and intact Langerhans islands with preserved contour and architecture (Fig. 5II(A)). The STZ group showed disruption, destruction, and atrophic changes in the Langerhans islands, while the acini appeared normal (Fig. 5II(B)). The insulin group exhibited hyperplasia of beta cells in the Langerhans islands (Fig. 5I (C)). The MNPI group displayed a compressed and decreased size of the typical Langerhans islands (Fig. 5II(D)). In the AlMPI group, the islets were compressed with mature infiltrate cellular components (Fig. 5II(E)). The ZNPI group resembled the STZ group in terms of pancreatic changes (Fig. 5I(F)). The MCPI group showed nearly non-injurious islets with hyperplasia of cellular content (Fig. 5I(G)).

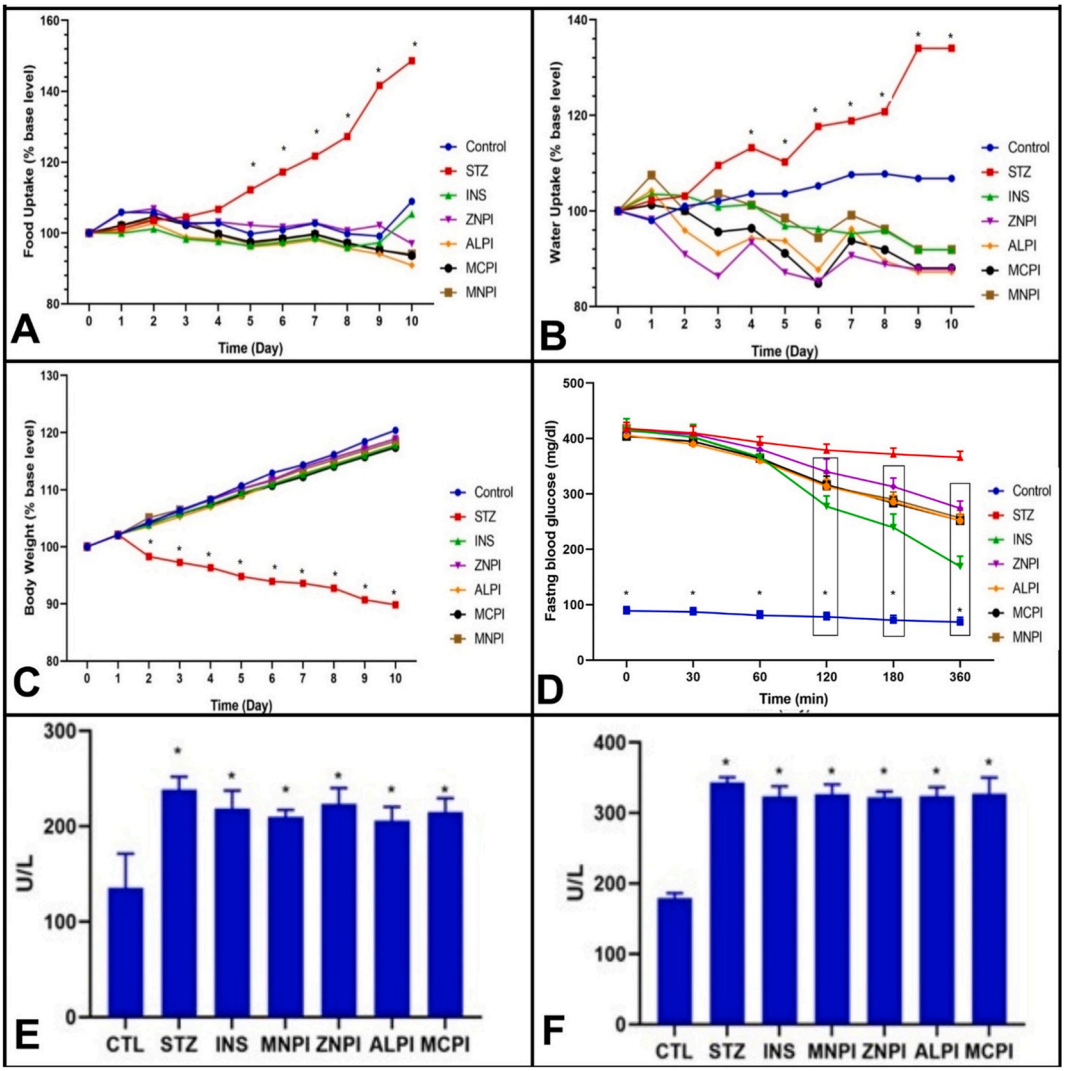

Fig. 4. Diabetic Rats' fasting blood glucose levels (Mean ± SD, n = 7) during 6 h after treatment with insulin and oral MSN form of insulin in comparison with a control group and also we checked long-term toxicity and efficacy of three types of nanoparticle administration on (A) Food uptake. (B) Amounts of drinking. (C) Bodyweight and (D) fasting blood glucose during 6 h after treatment with insulin and oral MSN form of insulin beside enzymatic activity (E) ALT and (F) AST of the liver. MSN form of insulin compares diabetic rat (STZ group), insulin (INS), Amin-grafted MSN/PEG/Insulin (MNPI), Al-grafted MSN/PEG/Insulin (AlMPI), Zinc-grafted MSN/PEG/Insulin (ZNPI), Co-grafted MSN/PEG/Insulin (MCPI). (*: Significant difference between oral insulin solution and STZ ($p < 0.001$)).

An efficient and non-toxic oral insulin delivery system could revolutionize the management of type 1 diabetes for patients, providing them with greater ease and comfort in controlling their blood glucose levels compared to traditional methods [31,32]. This study aimed to achieve two goals. Firstly, it involved the application of MSN for the fabrication of an insulin delivery system for the first time. Secondly, it examined the efficacy of this insulin delivery system in diabetic rats and its potential long-term side effects.

Type 1 diabetes was induced in rats through STZ injection, which was confirmed by an increase in fasting blood sugar, food and water intake, weight loss, and injuries to the liver and pancreas. Following the oral administration of MSN forms of insulin, fasting blood glucose levels in T1D rats reached their minimum levels within 5 h. By the 6th hour after administration, this effect was approximately equivalent to a 50% reduction in blood sugar compared to injectable insulin. Additionally, 10 days of consuming MSN forms of insulin was associated with reduced blood sugar levels, decreased food and water intake, improved weight gain, and preservation of the liver and pancreas structures.

An oral insulin delivery system holds the potential to alleviate the psychological challenges associated with daily insulin injections for individuals with diabetes. However, despite numerous studies, there are very few oral insulin delivery systems that are easily degradable, have low toxic effects, and are responsive to various digestive enzymes. Another challenge is the resistance of carriers to pH changes during the digestive process, which transitions from 1.2 in the stomach to 7.4 in the intestine [33,34].

Several methods exist to protect insulin from the effects of digestive enzymes and pH changes, and one of these solutions involves

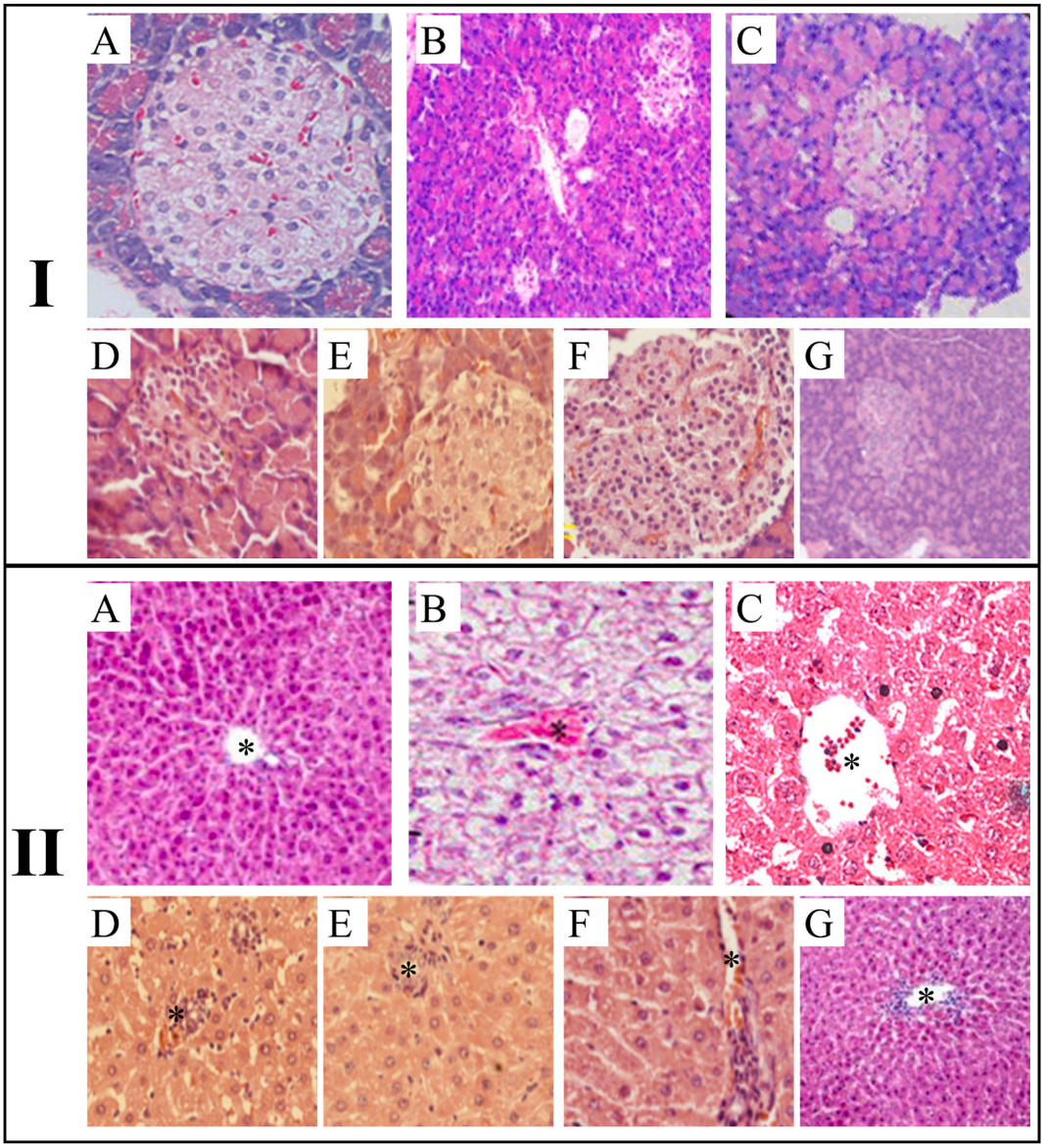

Fig. 5. Histopathology of the pancreas and liver in experimental groups after 10 days of treatment (H&E) (40X). **I** pancreas (A) control; normal parenchymal tissue, (B) diabetic group (STZ); degenerative and necrosis changes of lobule, (C) insulin (INS); dispersed degenerative and necrosis changes of hepatocytes (D) Amin-grafted MSN/PEG/Insulin (MNPI); some moderate changes like INS group (E) Al-grafted MSN/PEG/Insulin (AlMPI); moderate changes of hepatocytes (F) Zinc-grafted MSN/PEG/Insulin (ZNPI); mild hydropic degeneration changes of hepatocytes (G) Co-grafted MSN/PEG/Insulin (MCPI); look like the STZ group. **II.** liver (A) control; normal structure of Langerhans islands, (B) diabetic group (STZ); reduction of size and damaged in beta cells, (C) insulin (INS); some moderate anthropic changes in beta cells (D) Amin-grafted MSN/PEG/Insulin (MNPI); some moderate changes like INS group (E) Al-grafted MSN/PEG/Insulin (AlMPI); moderate changes look like INS group (F) Zinc-grafted MSN/PEG/Insulin (ZNPI); look like normal control group with hypertrophic cell (regeneration?) (G) Co-grafted MSN/PEG/Insulin (MCPI); look like STZ group with some sign of atrophy and decrease size of Langerhans islands.

encapsulating insulin in various nanoparticle coatings. Among these nanoparticles, the MSN form of oral insulin has demonstrated effective protection against changes during the digestive process due to its unique shape. As demonstrated by this study and previous research, the addition of different factors can enhance the absorption of insulin in the gastrointestinal tract [33,35]. In the present study, the addition of NH2 groups significantly improved insulin absorption.

Silica nanoparticles have been utilized since 1971 for carrying inorganic drugs. Among silica nanoparticles, MSNs, including the SBA (Santa Barbara Amorphous) [36], MCM (Mobil Composition of Matter) [37], and MCF (Mesocellular Foam) series [38]. Medical fields, including diagnostics, engineering, and therapy, have extensively explored the use of MSN in research. Among the different routes of administration, oral delivery utilizing MSN has emerged as a highly promising approach and has been extensively

investigated for the delivery of drugs and proteins, with insulin being of particular interest. Nanoparticles can effectively load high concentrations of insulin and its nano-suspension [39]. Orally administered MSN insulin effectively reduced blood glucose levels in diabetic rats after 6 h of treatment. Due to insulin's vulnerability to degradation in the stomach, it is necessary to protect it using different structures and carriers. In comparison to subcutaneous injections, which have a rapid and noticeable effect on blood sugar levels, oral insulin exerts its effect more gradually.

Considering that high blood sugar is the most important symptom of diabetes and insulin injection is the critical factor in controlling blood sugar in diabetic patients, insulin plays a vital role in carbohydrate metabolism [40]. Examining the long-term effects of the insulin delivery system, including toxicity assessment and quantification of tissue glycogen, as well as improving overall diabetes symptoms, can help prevent adverse effects associated with this treatment.

The newly designed chitosan-based MSN has demonstrated significant effects on glycemic control in diabetic rats. The administration of these drugs through gavage did not result in any specific clinical signs and had fewer side effects compared to the diabetic control group. They have not shown any negative effects.

Our results also indicate that liver enzymatic activity in diabetic rats changed due to the effect of STZ on liver structure. This study supports previous reports that co-treatment of insulin and the oral form of insulin does not affect liver enzymatic activity in diabetic animals. From an economic perspective, it is worth mentioning that the synthesis of these nanocomposites is relatively cost-effective because the materials used are made from inexpensive chemicals. Furthermore, despite the high efficiency of these nanocomposites in reducing blood sugar, the nanocomposite containing aluminum species can also lower blood sugar levels and aid in pancreas repair.

3.3. Molecular docking studies related to insulin and IR

To gain a deeper understanding of the interaction between our target set of four compounds and the active site of insulin and the IR, we conducted docking modeling studies using MVD. The results of the docking analysis can be found in Tables 2 and 3. The confirmation of the docked MSN compounds with insulin and the IR was evaluated based on their Total Energy or MolDock Score values, which predominantly exhibited negative energy values. This suggests that the compounds' binding effects occurred spontaneously and without external influence. Table 2 shows the docked conformation of the compounds with the related parameters. The values of Free Total Energy of MolDock Score-bind number were −308.171, −260.130, −197.867, and −124.352 for Co-grafted MSN, Zn-grafted MSN, Amin-grafted MSN, and Al-grafted MSN docked to insulin, respectively. The data in Table 3 show that the MolDock score-number of binding of Co-grafted MSN, Zn-grafted MSN, Al-grafted MSN, and Amin-grafted MSN interacted with IR was −337.608, −312.292, −297.545, and −214.362, respectively. The calculated minimum relative free total energy values score of the binding suggests that they reasonably bind to macromolecules. They were comparing the free total energy or MolDock score and several binding of compounds with insulin and IR that Co-grafted MSN was more effective than other compounds to insulin and IR.

Figs. 6 and 7 exhibit the strong binding of the ligands to the active sites of insulin and the IR. Specifically, in Fig. 6A-D, we observe significant interactions between the MSN compounds and the active site of insulin. The docking analysis data reveals that Co-grafted MSN forms van der Waals interactions, conventional hydrogen bonds, and unfavorable bumps with specific amino acids of insulin (PDB ID: 6jk8), namely Ile 2, Val 3, Gln 5, Asn 18, and Tyr 19 (Fig. 6A). Similarly, Zn-grafted MSN demonstrates van der Waals interactions, conventional hydrogen bonds, carbon hydrogen bonds, and unfavorable bumps with amino acid residues Ile 2, Gln 15, Asn 18, Tyr 14, and Tyr 19 within the active site of insulin (Fig. 6B). Additionally, Amin-grafted MSN forms van der Waals and carbon hydrogen bonds predominantly with Ser 12 in Fig. 6C. Lastly, Al-grafted MSN and insulin exhibit van der Waals interactions, conventional hydrogen bonds, carbon hydrogen bonds, and unfavorable bumps involving amino acid residues Gly 1, Ile 2, Val 3, Gln 5, Gln 15, Asn 18, and Tyr 19 (Fig. 6D).

Fig. 7A–D indicates MSN compounds embedded in the active site of IR (PDB ID: 4ZXB). Furthermore, Co-grafted MSN in Fig. 7A displayed Waals, Conventional Hydrogen Bond, Pi-Donor Hydrogen Bond, Unfavorable Donor-Donor, and Unfavorable Bumps with Gly 10, Gly 31, Glu 30, His 32, Asp 59, Cys 274, His 275, Tyr 277, Glu 287, Lys 310, Cys 312, His 313 and Glu 329 to IR respectively. Zn-grafted MSN was docked into IR using Cys 274, His 275 and Tyr 277, His313, Leu 314, Leu 315, Glu 316, Thr 325, Gln 328, Glu 329

Table 2
Resulted parameters from the interaction between MSN compounds and insulin.

Compound	Mol dock Score	Hbond	E_T (Ligand)	E_T
Co-MSN	−308.171	−4.341	−301.593	−35.969
Zn-MSN	−260.130	−0.916	−286.088	−270.028
MSN-NH_2	−197.863	−4.332	−206.11	−76.375
Al-MSN	−124.352	−4.648	−128.260	−180.30

Table 3
Resulted parameters from the interaction between MSN compounds and insulin Receptor.

Compound	Mol dock Score	Hbond	E_T (Ligand)	E_T
Co-MSN	−337.608	−23.578	−331.418	−65.92
Zn-MSN	−312.291	−23.951	−322.542	−311.581
Al-MSN	−297.545	−7.623	−310.221	−309.060
MSN-NH_2	−214.362	−8.195	−220.827	−202.954

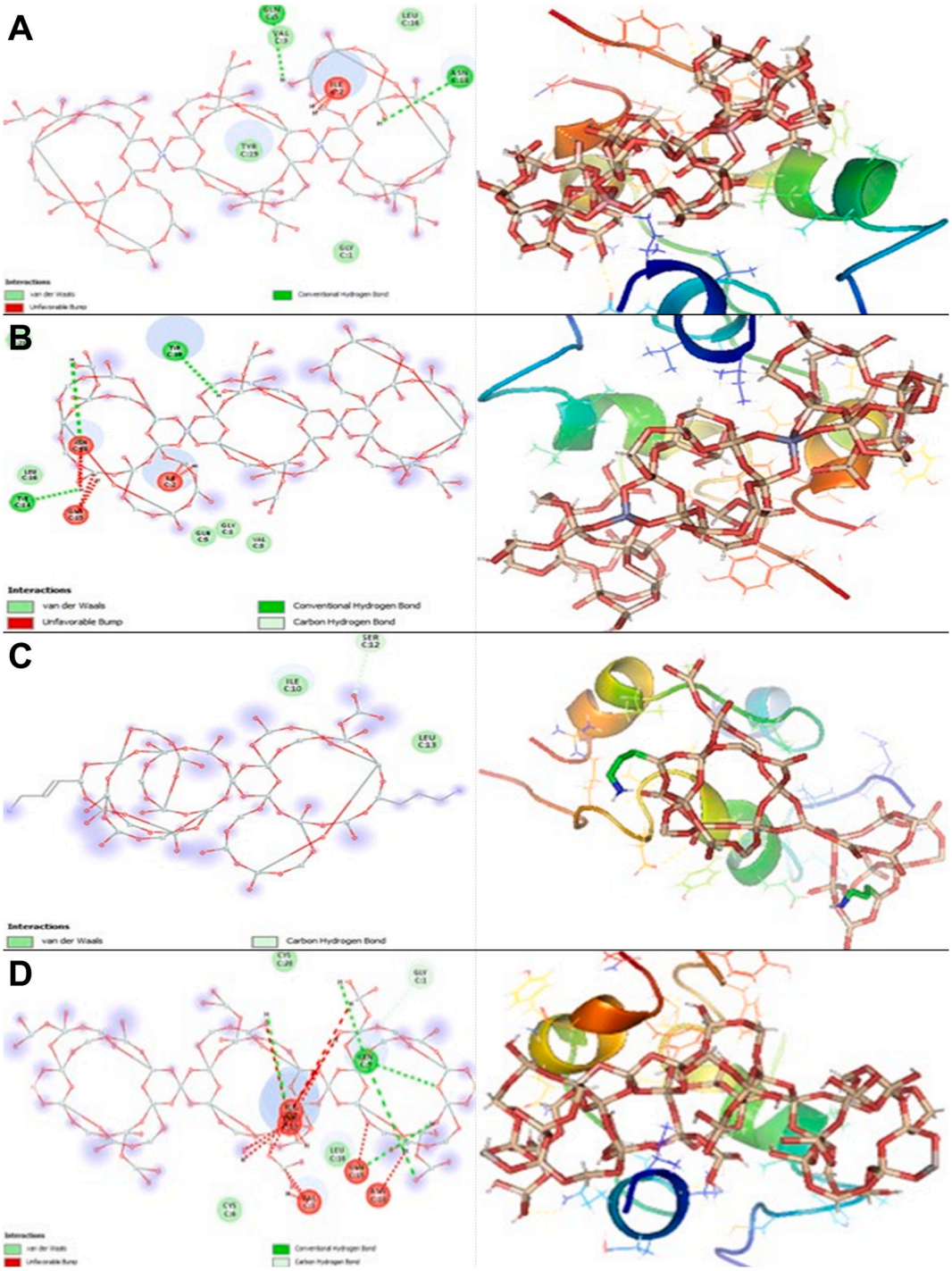

Fig. 6. Interactions between the mesosprus silica nanoparticle (MSN) compounds and the active site of insulin (A) Co-grafted MSN (B) Zn-grafted MSN (C) Amin-grafted MSN (D) AL-grafted MSN ligand maps and the best score docking solutions of MSN compounds and insulin with the selected crystal structure of 6KJ8.

and Arg 331 by van der Waals, Conventional Hydrogen Bond, Carbon Hydrogen Bonds, Pi-Donor Hydrogen Bond, Pi-Lone Pair and Unfavorable Bumps (Fig. 7B). Moreover, as demonstrated in Fig. 7C Al-grafted MSN/IR complex makes van der Waals, Conventional Hydrogen Bond, Pi-Donor Hydrogen Bond and Unfavorable Bumps with Cys 274, His 275, Glu 287, Cys 288, Pro 289, Ser 290, Lys 310, Glu 329 and Leu 330. The residues of IR like Arg 86, Cys 266, Cys 274, His 275, Cys 286, Cys 288, and Ser 290 interact by van der Waals, Conventional Hydrogen Bond, Carbon Hydrogen Bonds, and Unfavorable Bumps with Amin-grafted MSN (Fig. 7D).

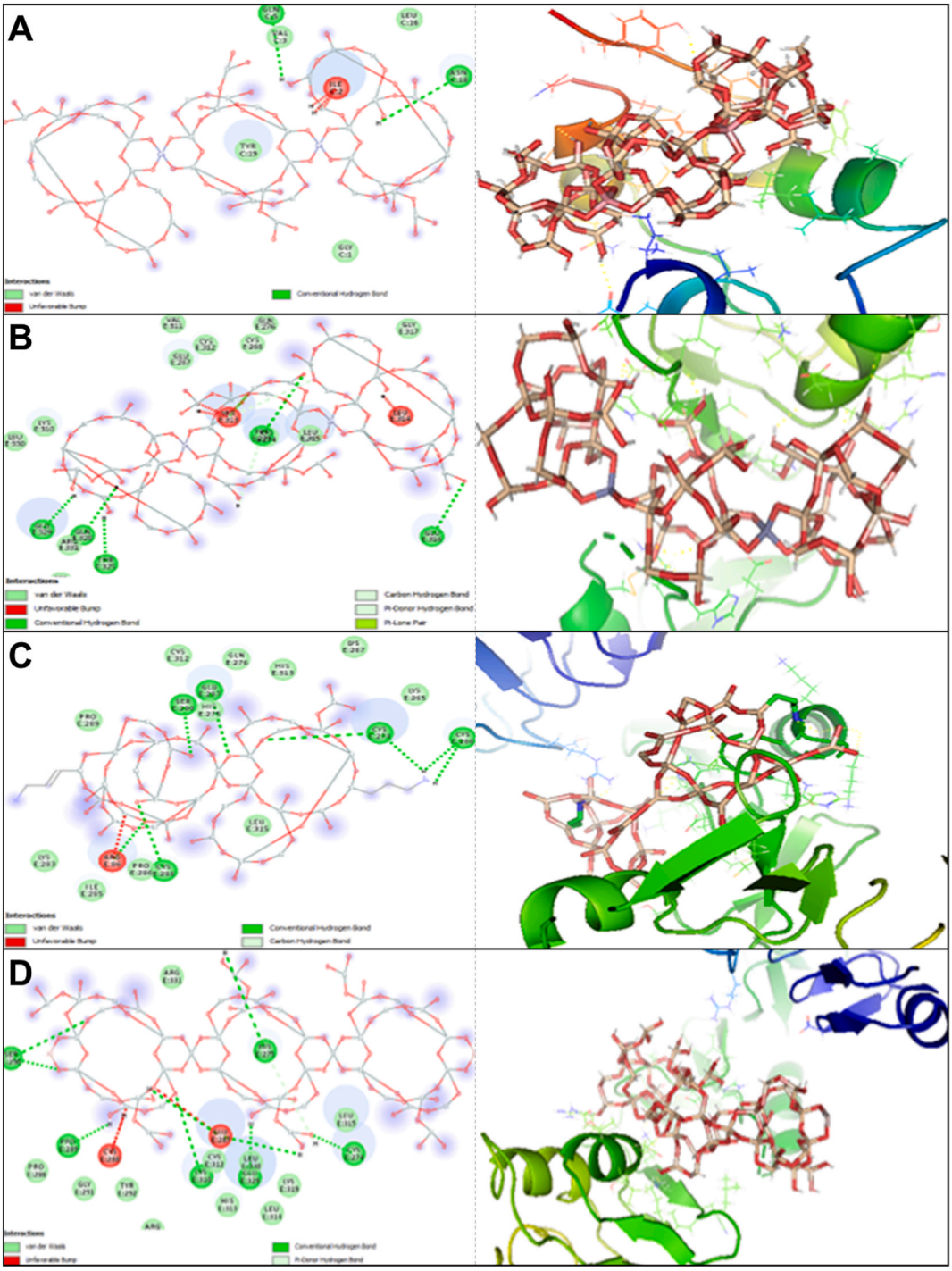

Fig. 7. MSN compounds embedded in the active site of insulin receptors (PDB ID: 4ZXB) (A) Co-grafted MSN (B) Zn-grafted MSN (C) Amin-grafted MSN (D) AL-grafted MSN ligand maps and the best score docking solutions of MSN compounds and insulin receptor with the selected crystal structure of 4ZXB.

Our *in-silico* studies based on Amin-grafted MSN, Al-grafted MSN, Zn-grafted MSN, and Co-grafted MSN that molecular docking study against insulin and IR was assessed. In general, if the amount of covalent, conventional H-bonds and steric interactions between the ligand and the protein is higher, that compound is a better target as a drug. Therefore, according to the parameters in Tables 2 and 3 and the existing total and interactions, Co-grafted MSN was selected as the best ligand for insulin and IR. The evaluation results by comparing the parameters of the result from MVD software showed that Co-grafted MSN in combination with insulin and IR is more

critical than other ligands and can be exhibited a better drug effect.

3.4. Advantages of this study in comparison to the other samples

Research on the oral delivery of antidiabetic peptides involves important strategies that include the incorporation of polymers, lipids, liposomes, and enzyme inhibitors into nanomaterial structures. Various insulin release techniques have been investigated to increased the oral bio-solubility of insulin drugs. These approaches work by safeguarding the peptides against enzymatic degradation within the gastrointestinal tract and facilitating their transport across intestinal cell barriers.

The results of this study demonstrate that the PEGylation method, combined with metal nanoparticles, offers significant advantages over other techniques as an efficient strategy for oral peptide delivery. Additionally, this study introduces a novel approach in the oral insulin pathway by utilizing metal-incorporated MSN encapsulated with the PEGylation process.

However, there are some inherent limitations associated with synthesizing oral insulin composites. These limitations include low drug loading, limited stability of nanomaterials in the acidic environment of the stomach, drug leakage, high production costs of nanocomposite products, lack of interaction with target tissues, low insulin release, the occurrence of side effects, and disruption of drug digestion processes after administering these oral drugs.

4. Conclusion

The nanocomposites of CMPI, AMPI, AlMPI, and ZMPI were synthesized from the initial MSN by loading metals, PEG, and insulin. These composites were characterized using XRD, FTIR, SEM, nitrogen sorption methods, and zeta potential measurement. The introduction of metals such as Co, Zn, and Al, as well as organic compounds, into pure MSN resulted in reduced crystallinity of the mesoporous structures. Furthermore, these nanomaterials exhibited lower surface area and pore volume compared to pristine MSN due to the incorporation of inorganic and organic compounds into the MSN structure.

The effective delivery of insulin through oral administration remains a significant clinical challenge, and despite extensive research on this subject, there is currently no available oral formulation for insulin. This study presents a novel approach for orally administering insulin, aiming to regulate blood glucose levels and alleviate liver and pancreas damage under both pathological and physiological conditions. By formulating insulin and encapsulating it within a mesoporous silica system, a substantial and durable reduction in blood glucose levels was achieved. The use of this multifunctional delivery system for oral insulin holds promising clinical potential in diabetes management, as it provides an oral route for insulin administration, preserves physiological activity, and facilitates insulin metabolism. Nonetheless, further investigation is required to advance this innovative formulation for future clinical trials.

Computational studies revealed that Co-grafted MSN exhibited higher binding affinity to insulin and IR compared to insulin alone. The calculated ligand energy and MolDock Score of the investigated compounds indicated good reactivity towards insulin and IR. Additionally, the compounds were docked into the active site of insulin and IR. Co-grafted MSN, the best-selected ligand, exhibited stronger binding affinity to insulin and IR compared to similar ligands.

Data availability

Data included in article/tables/figures. Material/referenced in article. Any other information will be made available on request.

CRediT authorship contribution statement

Ehsan Salarkia: Writing – original draft, Validation, Software, Methodology, Conceptualization. **Mahdis Mehdipoor:** Methodology. **Elahe Molaakbari:** Writing – original draft, Software. **Ahmad Khosravi:** Writing – original draft, Project administration, Conceptualization. **Mohammad Reza Sazegar:** Project administration, Methodology, Investigation. **Zohreh Salari:** Resources, Investigation. **Iman Rad:** Visualization. **Shahriar Dabiri:** Visualization. **Siyavash Joukar:** Writing – review & editing, Conceptualization. **Iraj Sharifi:** Writing – review & editing. **Guogang Ren:** Writing – review & editing, Formal analysis, Conceptualization.

Declaration of competing interest

The authors declare that they have no known competing financial interests or personal relationships that could have appeared to influence the work reported in this paper.

Acknowledgment

The authors would like to thank from Kerman University of Medical Sciences for supporting this research (Grant ID 9800446) and Department of Chemistry, North Tehran Branch, Islamic Azad University for helping to carry out this research.

Appendix A. Supplementary data

Supplementary data to this article can be found online at https://doi.org/10.1016/j.heliyon.2023.e20430.

References

[1] International Diabetes Federation, Diabetes Atlas, 2022. https://www.diabetesatlas.org/en/.
[2] H.P. Vemana, V. V Dukhande, Recent advances in the application of nanomedicine for the treatment of diabetes, Nanomedicine 17 (2022) 65–69.
[3] A. Al-Shwaheen, A.A.A. Aljabali, G. Alomari, M. Al Zoubi, W. Alshaer, B. Al-Trad, M.M. Tambuwala, Molecular and cellular effects of gold nanoparticles treatment in experimental diabetic myopathy, Heliyon 8 (2022).
[4] R.I.G. Holt, J.H. DeVries, A. Hess-Fischl, I.B. Hirsch, M.S. Kirkman, T. Klupa, B. Ludwig, K. Nørgaard, J. Pettus, E. Renard, The management of type 1 diabetes in adults. A consensus report by the American Diabetes Association (ADA) and the European Association for the Study of Diabetes (EASD), Diabetes Care 44 (2021) 2589–2625.
[5] V. Sugumar, K.P. Ang, A.F. Alshanon, G. Sethi, P.V.C. Yong, C.Y. Looi, W.F. Wong, A comprehensive review of the evolution of insulin development and its delivery method, Pharmaceutics 14 (2022) 1406.
[6] G. Iyer, S. Dyawanapelly, R. Jain, P. Dandekar, An overview of oral insulin delivery strategies (OIDS), Int. J. Biol. Macromol. 208 (2022) 565–585.
[7] Y. Zhang, J. Yu, A.R. Kahkoska, J. Wang, J.B. Buse, Z. Gu, Advances in transdermal insulin delivery, Adv. Drug Deliv. Rev. 139 (2019) 51–70.
[8] A. Elsayed, M. Al-Remawi, N. Jaber, K.M. Abu-Salah, Advances in buccal and oral delivery of insulin, Int. J. Pharm. (2023), 122623.
[9] H. Wu, J. Nan, L. Yang, H.J. Park, J. Li, Insulin-loaded liposomes packaged in alginate hydrogels promote the oral bioavailability of insulin, J. Contr. Release 353 (2023) 51–62.
[10] H. Pang, X. Huang, Z.P. Xu, C. Chen, F.Y. Han, Progress in oral insulin delivery by PLGA nanoparticles for the management of diabetes, Drug Discov. Today (2022), 103393.
[11] F. Mohamed, M.K. Oo, B. Chatterjee, B. Alallam, Biocompatible supramolecular mesoporous silica nanoparticles as the next-generation drug delivery system, Front. Pharmacol. 13 (2022), 886981.
[12] N. Sreeharsha, M. Philip, S.S. Krishna, V. Viswanad, R.K. Sahu, P.N. Shiroorkar, A.H. Aasif, S. Fattepur, S.M.B. Asdaq, A.B. Nair, Multifunctional mesoporous silica nanoparticles for oral drug delivery, Coatings 12 (2022) 358.
[13] M.R. Sazegar, A.A. Jalil, S. Triwahyono, R.R. Mukti, M. Aziz, M.A.A. Aziz, H.D. Setiabudi, N.H.N. Kamarudin, Protonation of Al-grafted mesostructured silica nanoparticles (MSN): acidity and catalytic activity for cumene conversion, Chem. Eng. J. 240 (2014) 352–361.
[14] Y. Gao, Y. He, H. Zhang, Y. Zhang, T. Gao, J.-H. Wang, S. Wang, Zwitterion-functionalized mesoporous silica nanoparticles for enhancing oral delivery of protein drugs by overcoming multiple gastrointestinal barriers, J. Colloid Interface Sci. 582 (2020) 364–375.
[15] Z. Xi, E. Ahmad, W. Zhang, J. Li, A. Wang, N. Wang, C. Zhu, W. Huang, L. Xu, M. Yu, Dual-modified nanoparticles overcome sequential absorption barriers for oral insulin delivery, J. Contr. Release 342 (2022) 1–13.
[16] J. Pradhan, S. Panchawat, Molecular docking studies and pharmacophore modeling of some insulin mimetic agents from herbal sources: a rational approach towards designing of orally active insulin mimetic agents, Curr. Tradit. Med. 6 (2020) 121–133.
[17] M.C. Lawrence, Understanding insulin and its receptor from their three-dimensional structures, Mol. Metab. 52 (2021), 101255.
[18] N.S. Kirk, Q. Chen, Y.G. Wu, A.L. Asante, H. Hu, J.F. Espinosa, F. Martínez-Olid, M.B. Margetts, F.A. Mohammed, V. V Kiselyov, Activation of the human insulin receptor by non-insulin-related peptides, Nat. Commun. 13 (2022) 5695.
[19] R.-R. Flörke, K. Schnaith, W. Passlack, M. Wichert, L. Kuehn, M. Fabry, M. Federwisch, H. Reinauer, Hormone-triggered conformational changes within the insulin-receptor ectodomain: requirement for transmembrane anchors, Biochem. J. 360 (2001) 189–198.
[20] J. Nielsen, J. Brandt, T. Boesen, T. Hummelshøj, R. Slaaby, G. Schluckebier, P. Nissen, Structural investigations of full-length insulin receptor dynamics and signalling, J. Mol. Biol. 434 (2022), 167458.
[21] M. Roy, A. Roy, S. Rustagi, N. Pandey, An overview of nanomaterial applications in pharmacology, BioMed Res. Int. 2023 (2023).
[22] R. Yang, G. Zhao, B. Cheng, B. Yan, Identification of potential matrix metalloproteinase-2 inhibitors from natural products through advanced machine learning-based cheminformatics approaches, Mol. Divers. 27 (2023) 1053–1066.
[23] A.A. Adeniyi, P.A. Ajibade, An insight into the anticancer activities of Ru (II)-based metallocompounds using docking methods, Molecules 18 (2013) 10829–10856.
[24] R. Thomsen, M.H. Christensen, MolDock, A new technique for high-accuracy molecular docking, J. Med. Chem. 49 (2006) 3315–3321.
[25] H. Tavakkoli, R. Attaran, A. Khosravi, Z. Salari, E. Salarkia, S. Dabiri, S.S. Mosallanejad, Vascular alteration in relation to fosfomycine: in silico and in vivo investigations using a chick embryo model, Biomed. Pharmacother. 118 (2019), 109240.
[26] O. Akhavan, M. Abdolahad, Y. Abdi, S. Mohajerzadeh, Silver nanoparticles within vertically aligned multi-wall carbon nanotubes with open tips for antibacterial purposes, J. Mater. Chem. 21 (2011) 387–393.
[27] N.G. Hajiagha, A. Mahmoudi, M.R. Sazegar, M.M. Pouramini, Synthesis of cobalt-modified MSN as a model enzyme: evaluation of the peroxidatic performance, Microporous Mesoporous Mater. 274 (2019) 43–53.
[28] M.R. Sazegar, A. Dadvand, A. Mahmoudi, Novel protonated Fe-containing mesoporous silica nanoparticle catalyst: excellent performance cyclohexane oxidation, RSC Adv. 7 (2017) 27506–27514.
[29] E. Juère, R. Caillard, D. Marko, G. Del Favero, F. Kleitz, Smart protein-based formulation of dendritic mesoporous silica nanoparticles: toward oral delivery of insulin, Chem. Eur J. 26 (2020) 5195–5199.
[30] X. Tan, X. Liu, Y. Zhang, H. Zhang, X. Lin, C. Pu, J. Gou, H. He, T. Yin, Y. Zhang, Silica nanoparticles on the oral delivery of insulin, Expet Opin. Drug Deliv. 15 (2018) 805–820.
[31] S. Sarkar, M. Ekbal Kabir, J. Kalita, P. Manna, Mesoporous silica nanoparticles: drug delivery vehicles for antidiabetic molecules, Chembiochem (2023), e202200672.
[32] A. Abdel-Moneim, H. Ramadan, Novel strategies to oral delivery of insulin: current progress of nanocarriers for diabetes management, Drug Dev. Res. 83 (2022) 301–316.
[33] H. Zhang, Z. Gu, W. Li, L. Guo, L. Wang, L. Guo, S. Ma, B. Han, J. Chang, pH-sensitive O-carboxymethyl chitosan/sodium alginate nanohydrogel for enhanced oral delivery of insulin, Int. J. Biol. Macromol. 223 (2022) 433–445.
[34] S.K. Panigrahy, A. Kumar, Biopolymeric nanocarrier: an auspicious system for oral delivery of insulin, J. Biomater. Sci. Polym. Ed. 33 (2022) 2145–2164.
[35] H. Spleis, M. Sandmeier, V. Claus, A. Bernkop-Schnürch, Surface design of nanocarriers: key to more efficient oral drug delivery systems, Adv. Colloid Interface Sci. (2023), 102848.
[36] C. Romere, C. Duerrschmid, J. Bournat, P. Constable, M. Jain, F. Xia, P.K. Saha, M. Del Solar, B. Zhu, B. York, Asprosin, a fasting-induced glucogenic protein hormone, Cell 165 (2016) 566–579.
[37] C. Xu, C. Lei, C. Yu, Mesoporous silica nanoparticles for protein protection and delivery, Front. Chem. 7 (2019) 290.
[38] Y. Yang, S. Chen, Y. Liu, Y. Huang, K.-L. Cheong, B. Teng, W. Liu, Long-term treatment of polysaccharides-based hydrogel microparticles as oral insulin delivery in streptozotocin-induced type 2 diabetic mice, Biomed. Pharmacother. 133 (n.d.) 110941..
[39] M. Shokri, H. Faridnouri, A. Ghasemi, Effects of long-term administration of oral sodium nitrate on liver enzyme concentrations in type 2 diabetic male rats, Iran, J. Endocrinol. Metab. 22 (2020) 1–10.
[40] M.E. El-Naggar, F. Al-Joufi, M. Anwar, M.F. Attia, M.A. El-Bana, Curcumin-loaded PLA-PEG copolymer nanoparticles for treatment of liver inflammation in streptozotocin-induced diabetic rats, Colloids Surfaces B Biointerfaces 177 (2019) 389–398.